Delay Time of Hemoglobin S Polymerization Prevents Most Cells from Sickling in Vivo

ANDREA MOZZARELLI, JAMES HOFRICHTER, WILLIAM A. EATON*

A laser photolysis technique has been developed to assess the quantitative significance of the delay time of hemoglobin S gelation to the pathophysiology of sickle cell disease. Changes in the saturation of hemoglobin S with carbon monoxide produced by varying the intensity of a photolytic laser beam were used to simulate changes in the saturation of oxyhemoglobin S produced by variations in oxygen pressure. The presence of polymer at steady-state saturation with carbon monoxide was determined by measurement of the kinetics of gelation after complete photodissociation. The kinetics are a very sensitive probe for polymer since small amounts of polymerized hemoglobin increase the rate of nucleation sufficiently to eliminate the delay period. First, the equilibrium gelation properties of partially photodissociated carbonmonoxyhemoglobin S were shown to be the same as partially oxygenated hemoglobin S, and the method was then used to determine the effect of saturation on the formation and disappearance of polymers in individual sickle cells. The saturation at which polymers first formed upon deoxygenation was much lower than the saturation at which polymers disappeared upon reoxygenation. The results indicate that at venous saturations with oxygen, gelation takes place in most cells at equilibrium, but is prevented from occurring in vivo because the delay times are sufficiently long that most cells return to the lungs and are reoxygenated before polymerization has begun.

THE POLYMERIZATION OF HEMOGLOBIN S UPON DEOXYgenation to form an extremely viscous or solid-like gel is the primary pathophysiological event in sickle cell disease. Gelation distorts the red cell and decreases its deformability. These rigid cells may obstruct the narrow vessels of the circulation, resulting in impaired oxygen delivery. Tissue hypoxia caused by vaso-occlusion in the microcirculation and the resulting organ damage constitute the principal cause of the morbidity and mortality of the disease (*1, 2*).

Studies on the gelation process in molecular, and even atomic detail (*2, 3–7*), have evolved to the point that it is possible to approach the problem of gelation in vivo and vaso-occlusion more rigorously (*7*). What information is necessary to accurately describe gelation within red cells in vivo? One would like to describe the distributions for individual cells in both the fractional saturation with oxygen and the amount of polymer at all points in the circulatory system. This description must accurately incorporate the kinetics of the polymerization process, which are, perhaps, the most interesting and unusual aspect of gelation. In a polymer-free solution, gelation is characterized by a pronounced delay period prior to the appearance of any polymerized hemoglobin (*8, 9*). The delay time is extraordinarily sensitive to solution conditions, particularly to the hemoglobin S concentration and the saturation with oxygen or carbon monoxide (*8–14*). The reciprocal of the delay time depends on the 15th to 50th power of the initial hemoglobin S concentration (*8, 11, 14*). These findings led to the proposal that the delay times for intracellular gelation, relative to the times required for red cells to traverse the microcirculation, are the primary determinant of severity in sickle cell disease (*7, 15*). This concept suggested that increasing the delay time, for example by decreasing the intracellular hemoglobin concentration, would allow more cells to escape the microcirculation before gelation begins, and should lead to amelioration of the disease (*7, 15*).

The population of sickle cells within a given patient is extremely heterogeneous because of differences in hemoglobin S concentration (*16*). For this reason, measurements must be performed on individual cells. The effects of cell heterogeneity are most evident in kinetics studies, where the delay times range from a few milliseconds to more than 100 seconds, with a delay time for most of the cells of less than the 1 second required for cells to pass through the microcirculation (*17*). In these experiments the initial saturation (with carbon monoxide) was 100 percent, while the saturation at which the kinetics of gelation were measured was close to zero. In vivo the situation is different because deoxygenation in the tissues is only partial, and therefore much longer delay times are expected. In addition, oxygenation in the lungs is not complete, so that some cells may contain residual polymerized hemoglobin at arterial oxygen saturations (*6, 7, 15, 18, 19*).

Until now there have been neither equilibrium nor kinetic data which describe gelation in single red cells at partial saturation with oxygen. In this article we describe our initial findings obtained with a new laser photolysis technique to detect the presence of polymer in individual cells as a function of saturation with carbon monoxide. We show, in addition, that carbon monoxide has the same effect on gelation in vitro as does oxygen. The results permit the first quantitative assessment of the role of the delay time in determining the proportion of cells containing polymerized hemoglobin S in the arterial and venous circulations of a patient with sickle cell disease.

Rationale of the experiment. The principal objectives of our measurements were to determine the saturation with oxygen in single red cells at which polymers first form upon deoxygenation, and the saturation at which they disappear on reoxygenation. We sought an experimental method that permitted the saturation to be

A. Mozzarelli was a Fogarty Research Fellow at the National Institutes of Health, Bethesda, MD 20892; his present address is Istituto di Biologia Molecolare, Universita di Parma, 43100 Parma, Italy. J. Hofrichter and W. A. Eaton are at the Laboratory of Chemical Physics of the National Institute of Diabetes and Digestive and Kidney Diseases at the National Institutes of Health.

*To whom correspondence should be addressed.

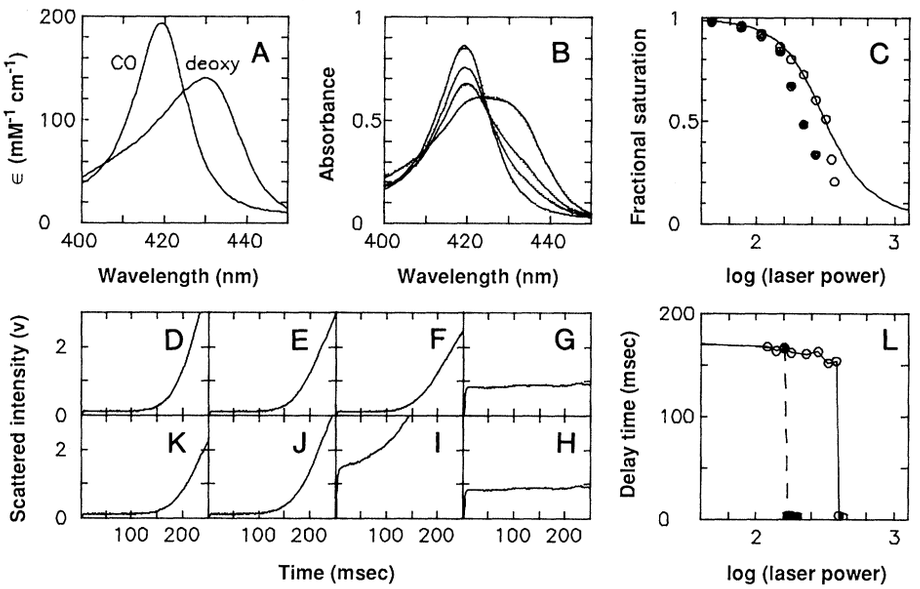

Fig. 1. Formation and disappearance of polymer in partially photolysed HbCO S solutions at 35°C. The preparative beam was obtained by focusing the 514-nm line of an argon ion laser to a 1/*e* diameter of 9.2 μm while, to reduce laser heating, the more intense probe beam was focused to a diameter of 2 μm, with a peak power of 0.7 kW/cm^2. Heating of the sample by the laser beams was estimated to be less than 0.5°C under all experimental conditions (*14*). (**A**) Optical spectra of HbCO A and deoxyHb A obtained by complete photodissociation with the preparative beam, which were measured with a microspectrophotometer (*21, 38*). These spectra were used as the reference spectra for calculating the fractional saturations in partially photolysed HbCO S. (**B**) Optical spectra of HbCO S [2.3-μm layer (0.329 g/ml) dialyzed against 0.15*M* potassium phosphate buffer, *p*H 7.35, plus 55 m*M* sodium dithionite] as a function of increasing power of the preparative beam. The points are the data, and the continuous curves are the least-squares fits to the points obtained from a linear combination of the spectra in (A). The fits are so good that the points are barely visible. (**C**) Fractional saturation with carbon monoxide obtained from least-squares fits to the spectra in (A) as a function of the logarithm of the incident power of the preparative beam when the sample is desaturated by increasing the laser power (open circles), or resaturated by decreasing the laser power once gelation had occurred (filled circles). The data coincide once depolymerization is complete. The solid curve is a theoretical fit to the open circles, excluding the two points at the highest power, as calculated from the two-state allosteric model for the power dependence of the saturation (*14*). (**D** to **K**) Kinetics of gelation at zero saturation measured from the forward scattered light of the probe beam (*21*) at various initial steady-state saturations produced by the preparative beam. (**D** to **G**) The power of the preparative beam was adjusted to produce an initial steady-state desaturation and, about 15 seconds later, the more intense probe beam was switched on to produce complete photodissociation and the kinetics were recorded. (**H** to **K**) The preparative beam was first turned on at a power just above that required to produce gelation within 15 seconds. After 15 seconds, the power was decreased and held fixed at a lower value for 45 seconds. We then measured the kinetics of gelation at zero saturation, using the probe beam. Both beams were switched off for at least 45 seconds between experiments to permit complete rebinding of carbon monoxide and degelation. The relative power in the preparative beam was 0 for (D) and (K), 160 for (E) and (J), 180 for (F) and (I), 400 for (G), and 430 for (H). (**L**) Delay time as a function of the logarithm of the power of the preparative beam in desaturation experiments (open circles) and resaturation experiments (filled circles).

easily controlled and accurately measured, as well as a probe that could detect the presence of intracellular polymers with high sensitivity. These criteria were satisfied by an experiment in which photolysis in the presence of excess carbon monoxide was used to control the saturation, and light scattering was used to detect polymerized hemoglobin. The experiment required two laser beams. One beam, called the preparative beam, had a diameter of about 10 μm and was used to create partially saturated hemoglobin S by continuous photodissociation of the carbon monoxide complex. Any desired steady-state saturation could be rapidly obtained by varying the incident laser intensity. The saturation was then determined by measuring the optical absorption spectrum of the sample with a microspectrophotometer. A second more intense beam, called the probe beam, with a diameter of about 2 μm, was used to detect polymer by measuring the kinetics of gelation from changes in the scattered light intensity after complete photodissociation of the remaining carbon monoxide (*14, 17, 20, 21*).

The design of this experiment draws on the results of earlier investigations of the kinetics of gelation. High-sensitivity light scattering experiments on thermally induced gelation of completely deoxygenated hemoglobin S showed that the delay time is shortened or even eliminated when very small amounts of polymerized hemoglobin are present (*22*). These results can be understood in terms of the double nucleation mechanism that explains all of the major observations on the kinetics of gelation (*5*). According to this mechanism, gelation is initiated by homogeneous nucleation of individual polymers in the bulk solution phase; but the reaction propagates by a second process, called heterogeneous nucleation, in which additional polymers nucleate on the surface of existing ones. As nucleation and polymerization proceed, there is an autocatalytic increase in the rate of heterogeneous nucleation because the polymer surface area on which these nuclei can form is continuously increasing. Since the rate of nucleation is initially very slow, there is a delay before any polymerized hemoglobin can be detected. In solutions that already contain even very small amounts of polymer, the initial rate of heterogeneous nucleation is increased, and the delay period is shortened or eliminated.

For the experiment to be relevant to the problem of gelation in vivo, the gelling behavior of carbonmonoxyhemoglobin S (HbCO S) partially saturated by continuous photodissociation must be very similar to that of partially saturated oxyhemoglobin S (HbO_2 S) obtained by lowering the oxygen pressure. We have reason to believe that this should be the case. In the absence of light, the equilibrium data on gelation are the same for the two ligands, as shown by a comparison of solubilities as a function of the solution phase saturation of the gel (*4, 12*). This finding can be explained with a simple extension of the two-state allosteric model, which postulates that ligands control gelation because only molecules in the T quaternary structure polymerize (*4*). Similarities in their binding properties can be used to argue that, at a given fractional saturation, the proportion of molecules that have the T quaternary structure is the same for the two ligands (*23*). Desaturation by photolysis is not expected to alter the dependence of the proportion of molecules in the T state on fractional saturation, since cooperativity in carbon monoxide binding curves, as judged by a comparison of Hill plots, is independent of light intensity (*24*). This is consistent with kinetic studies which show that cooperativity in carbon monoxide binding is primarily manifested in the overall association rate and is, therefore, only slightly affected by the increase in the overall dissociation rate caused by continuous photolysis (*24, 25*).

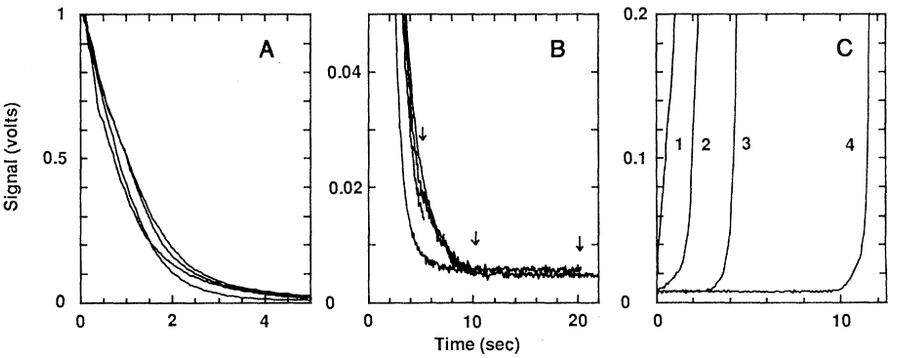

Fig. 2. Sensitivity of the kinetics of gelation to the presence of polymerized hemoglobin (sample 0.314 g/ml, at 35°C). After gelation of the sample produced by partial photolysis with the preparative beam, the power of the preparative beam was rapidly reduced to a value just below that at which the polymer completely disappears. The forward scattered intensity from the preparative beam is shown in (**A**), and on an expanded scale in (**B**). At various times after the decrease in power of the preparative beam, as is indicated by the arrows in (B), the power in the preparative beam was increased to the original value that produced gelation. The kinetic traces measured with the probe beam are shown in (**C**). Traces 1 to 4 correspond to times after decreasing the power of the preparative beam of 5, 10, 20, and 30 seconds, respectively. The delay time for this partially saturated sample was 7.7 ± 2.0 seconds in separate experiments at 100 percent initial saturation.

Critical saturation of hemoglobin S solutions. To determine whether gelation of partially photolysed HbCO S simulates gelation of partially saturated HbO_2 S, we first compared the solubility of partially photolysed HbCO S with previous data from sedimentation studies on partially saturated HbO_2 S. To do so we prepared a series of solutions of HbCO S at a pressure of 1 atmosphere carbon monoxide and at different protein concentrations. As the power of the preparative beam was increased or decreased, optical absorption spectra were measured and analyzed to determine the fractional saturation, and the kinetics of gelation was measured after complete photodissociation with the probe beam.

On decreasing the saturation by increasing the power of the preparative beam, the delay time remains constant until some well-defined saturation is reached (Fig. 1, E and F). This point is marked by a dramatic change in the kinetic progress curve reflecting the appearance of polymer, that is, the disappearance of the delay period and an increase in the initial light scattering signal (Fig. 1G). At the same laser power there is a sharp decrease in the fractional saturation (Fig. 1, B and C). Since the affinity of the hemoglobin S polymer is lower than that of molecules free in solution (*4, 12*), this decrease can be attributed to the polymerization of a substantial portion of the hemoglobin S. This observation is consistent with previous kinetic studies showing that the presence of the delay time causes the sample to pass from a state in which there is no polymer to one in which a significant amount of the hemoglobin has polymerized. This phenomenon arises because the hemoglobin S concentration must significantly exceed the solubility in order for gelation to occur on the same time scale as the experiment (*10*). For example, polymer does not appear in the 0.33 g/ml sample (Fig. 1) until the solution is desaturated to 50 percent, where sedimentation studies predict a solubility of only 0.22 g/ml, so that about 50 percent of the hemoglobin is expected to polymerize on gelation.

Once gelation had occurred, the sample was resaturated by decreasing the laser power of the preparative beam, and the spectra and kinetic progress curves were again measured at each power (Fig. 1, H and I). At some well-defined power, the kinetic progress curve suddenly recovers its original form and delay time (Fig. 1J). The saturation determined from the spectra at this power is the same as that found on desaturation (Fig. 1C). Both results are consistent with the absence of any polymerized hemoglobin.

The recovery of the original delay time is a sensitive indicator that depolymerization is complete. This fact was demonstrated by a series of experiments in which the intensity of the preparative beam illuminating a gelled sample was suddenly decreased to a power just below that at which the delay time was recovered (Fig. 2). The extent of depolymerization was monitored by measuring the scattered intensity from the preparative beam (Fig. 2, A and B). At various intervals after the decrease, the power of the preparative beam was again raised to its original value, and the kinetics of repolymerization was measured in the same way (Fig. 2C). The original delay time was not recovered until the scattered intensity decreased to less than about 0.05 percent of its original value, the minimal detectable level in the experiment. The results also show that depolymerization is complete in less than 30 seconds under these experimental conditions. Consequently, the difference between the saturation at which polymer appears in desaturation experiments and that at which polymer disappears in resaturation experiments must result from the delay time for polymerization, not from slow depolymerization.

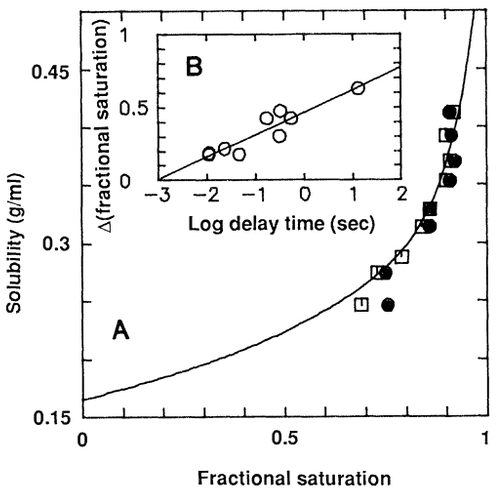

Fig. 3. Comparison of gelling data for partially photolysed HbCO S and partially saturated HbO_2 S. (**A**) Concentration as a function of critical saturation with carbon monoxide and solubility as a function of saturation with oxygen. The points are the results of photolysis experiments and show the saturation with carbon monoxide at which polymers disappear in samples of known concentration in resaturation experiments (that is, the "critical saturation"). The saturations were determined from the recovery of the delay time (closed circles) and the recovery of the solution fractional saturation (squares). The saturations measured in desaturation and resaturation experiments were assumed to be identical if they were within ±3 percent (see, for example, Fig. 1C) based on a root-mean-square error of ±2 percent in fitting the desaturation data to the theoretical binding curve. The curve is the solubility as a function of the fractional saturation with oxygen measured by Sunshine *et al.* (*4*), shifted downward by 0.018 g/ml to account for the lower solubility of deoxyhemoglobin S at 35°C. The solubility is defined as the total hemoglobin concentration in the supernatant after sedimentation of the polymers of the gel (*10*). (**B**) The difference between the saturations at which polymers form and disappear (hysteresis) in solution photolysis experiments. The difference is plotted as a function of the logarithm of the delay time for the samples in (A). The average value of the saturation of the kinetic and spectral methods was used. The line is a least-squares fit to the data points.

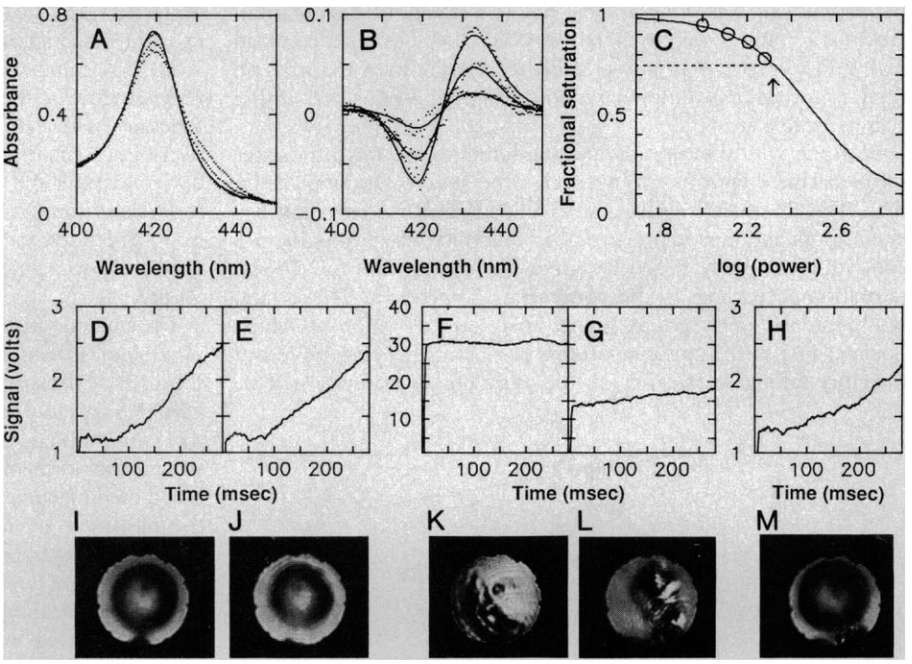

Fig. 4. Formation and disappearance of polymer in a partially photolyzed single sickle cell. The cells were suspended in a physiological buffer (95 m*M* NaCl, 20 m*M* KCl, 23.3 m*M* $NaHCO_3$, 1 m*M* Na_2HPO_4, 1 m*M* $MgCl_2$, 1 m*M* $CaCl_2$, 5 m*M* glucose, bovine serum albumin at 1 mg/ml), and saturated with a gas mixture of 95 percent carbon monoxide and 5 percent carbon dioxide. At the low hematocrit used in these experiments (0.1 percent) the 2,3-diphosphoglycerate levels are not diminished for at least 6 hours. The fetal hemoglobin level was 7 percent, close to the average for homozygous sickle cell patients. Other details of the experiment are the same as in the legend to Fig. 1. (**A**) Optical spectra at increasing power of the preparative beam. The continuous curve is a least-squares fit to the optical spectrum at 100 percent saturation. (**B**) Difference spectra from (A). The points are the spectrum measured under continuous illumination with the preparative beam minus the spectrum at 100 percent saturation. The curves are least-squares fits with difference spectra from the equation: $\Delta A(\lambda) = (1 - \alpha)[A_{Hb}(\lambda) - A_{HbCO}(\lambda)]$, where α is the fractional saturation with carbon monoxide, $A_{HbCO}(\lambda)$ is the fitted spectrum at 100 percent saturation in (A), and $A_{Hb}(\lambda)$ is the deoxyHb spectrum scaled to the same concentration and pathlength. (**C**) Fractional saturation determined from the least-squares fits in (B) as a function of the logarithm of the relative power in the preparative beam. The continuous curve is theoretical, as in Fig. 1C. The arrow indicates the power of the preparative beam at which deformation occurs, allowing the determination of the saturation by extrapolation of the theoretical curve. (**D** to **H**) Kinetics of gelation at relative incident powers of the preparative beam of 0 for (D), 130 for (E), 210 for (F), 130 for (G), and 120 for (H). (**I** to **M**) Optical micrographs at corresponding laser powers. The relatively poor quality of these micrographs is due to the use of the low numerical aperture of the substage objective (0.25), which was necessary to generate the large diameter of the preparative beam and to perform the spectral measurements on cells, as well as to the presence of scattered laser light. Nevertheless, they show that there is a large change in the shape of the cell upon loss and recovery of the delay time.

Complete depolymerization is sufficiently rapid so that the saturation at which the delay time is recovered may be considered an equilibrium value. We call this the "critical saturation," and it can be defined either as the maximum saturation at which polymer is present at equilibrium, or as the saturation at which the total hemoglobin concentration of the sample is equal to the solubility. Thus, the curve of the concentration as a function of the critical saturation measured in this study is equivalent to the curve of the solubility as a function of the solution phase saturation from previous sedimentation experiments (*4*) (Fig. 3). The excellent agreement between the two data sets (Fig. 3) is convincing evidence that the gelation properties of partially saturated HbO_2 S are the same as those for partially photolysed HbCO S.

Probing for polymer in single cells. Experiments on individual cells from a patient with homozygous sickle cell disease were carried out in the same way as those for solutions (Fig. 4). First, the optical spectra were measured as a function of increasing power of the preparative beam (Fig. 4, A to C) until there was a sudden, gross deformation of the cell (Fig. 4K), which prevented further spectral measurements. After these measurements were made, the preparative beam was turned off to permit complete resaturation with carbon monoxide and depolymerization. The cell was then probed for the presence of polymer by first adjusting the power of the preparative beam, and, about 15 seconds later, by measuring the kinetics of gelation after reducing the saturation to zero with the probe beam (Fig. 4, D to H). Between each measurement, both the preparative and probe beams were extinguished. In all cases, the delay time at zero saturation for undeformed cells is independent of the steady state saturation produced by the preparative beam. At the point at which cellular deformation occurs, the delay period disappears, and there is an initial increase in light scattering (Fig. 4, F and G) that is much larger than what is found for gels (Fig. 1, G to I). These results show that deformation is a reliable indicator of intracellular gelation. The same conclusion has been reached from micropipette experiments in which the static and dynamic rigidities of individual cells were measured as a function of decreasing oxygen pressure (*26*). In these studies undeformed cells always showed normal rheological properties, while deformed cells, with the exception of "smooth-surfaced irreversibly sickled cells," showed marked changes in both static and dynamic rigidities. These findings on the correspondence between gelation and cellular deformation prompted us to perform our experiments in which desaturation was carried out more rapidly (over a period of about 1 minute instead of 10 minutes), with visual observations of cell morphology at each laser power. In these experiments, the saturation at which cellular deformation occurs is always lower than what is found in the slower desaturation experiments.

Once the power in the preparative beam was sufficient to cause intracellular gelation and deformation, we decreased it over a period of about 1 minute in order to determine the critical saturation. The kinetic progress curves show no delay period until a well-defined power at which the cell rapidly returns to its normal biconcave disc shape. At this power, recovery of the normal cell shape (Fig. 4M) is accompanied by recovery of the original delay period (Fig. 4H). The saturation corresponding to this power is taken as the critical saturation for the particular cell. As with the solution experiments, the critical saturation is always higher than the saturation at which polymer first formed in desaturation experiments. Also, the critical saturation is the same for cells that were initially desaturated at the two different rates.

The complete experiment on a cell consisted of measuring the critical saturation and the saturation at which polymer forms at two different rates of desaturation. This experiment was performed on 26 different cells from the same patient. For an additional nine cells

the experiment was done at only the slower rate of desaturation. About 60 minutes were required to do a complete experiment on each cell, so that it was only possible to perform measurements on three cells from a given preparation during the 3-hour period that cells are stable at 35°C.

Both the critical saturation and the saturation at which polymer forms decrease with increasing delay time at zero saturation (Fig. 5A). This is expected since the dominant factor controlling the equilibrium and kinetic properties is the intracellular hemoglobin S concentration, with the delay time decreasing and the critical saturation increasing as the concentration increases. The critical saturation for every cell is higher than the saturation at which polymer first forms in the desaturation experiments (Fig. 5B), and the latter saturation is lower for the more rapid desaturation. This hysteresis (Fig. 5B) is similar to that observed in the solution experiments (Fig. 3B).

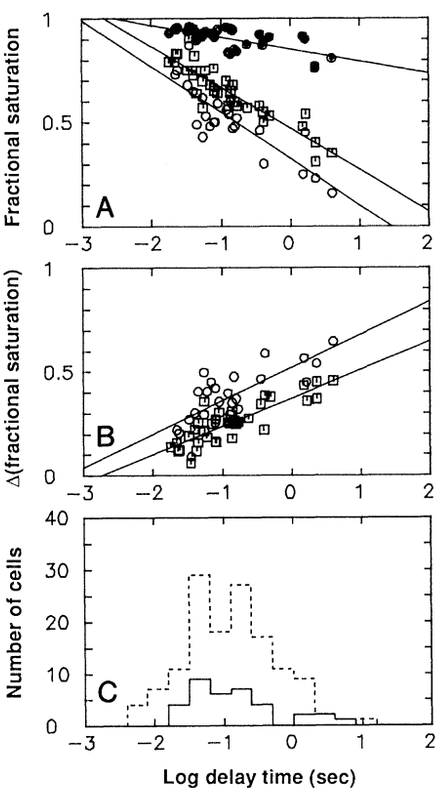

Fig. 5. Summary of cell data. All cells were chosen at random and were from the same patient. (**A**) Fractional saturation at which polymers form and disappear as a function of the logarithm of delay time at zero saturation. The squares are the saturations at which polymers form in desaturation experiments in which the power was decreased over a period of about 10 minutes while spectra were being measured. The open circles are the corresponding data obtained by desaturating in about 1 minute, and with cellular deformation as the only criterion for polymer formation. The filled circles are the critical saturations, that is the saturations at which polymers disappear in resaturation experiments, as judged by the reappearance of the original delay time. The lines are the least-squares fits to the data points. (**B**) Hysteresis in saturations at which polymers form and disappear. The saturation in the slow (10 minutes) (squares) and fast (1 minute) (open circles) desaturation experiments is subtracted from the critical saturation determined in resaturation experiments and plotted versus the delay time. The lines are least squares fits to the data points. (**C**) Distribution of delay times at zero saturation. The dashed histogram is for 140 cells from the same patient. In another 15 cells from this set of experiments, gelation did not occur at zero saturation with the probe beam (within the 2- to 5-minute period of the measurement). The solid histogram is for the 35 cells for which saturations where polymers form and disappear were measured (two cells did not sickle). The mean, median, and standard deviation for the 140-cell set was −0.86 (140 msec), −0.90 (130 msec), and 0.69, while the corresponding values for the 35-cell set were −0.88 (130 msec), −0.90 (130 msec), and 0.62. The medians included the cells that did not sickle.

To determine whether the results on the set of 35 cells are representative of the entire cell population, we measured only delay times for 140 cells from the same patient (Fig. 5C). The two distributions have nearly identical means, medians, and standard deviations, but the 35-cell set has somewhat fewer cells with very short delay times, which would correspond to high critical saturations. The F-test indicates that the 35-cell set and the 140-cell set do not belong to a different continuous distribution (significance level, 99 percent).

The data on saturations are summarized in a more useful form for physiological considerations in Fig. 6. Since the solution experiments show that partially saturated HbO_2 S and partially photolysed HbCO S have the same gelling behavior at the same saturation, and the solution-phase oxygen binding curve for hemoglobin S is the same as that for hemoglobin A (*4, 27*), we can use the normal whole blood binding curve to obtain the oxygen pressure corresponding to the measured saturations. Because cells containing polymer are deformed and undeformed cells contain no polymer, the fraction of cells containing polymer can be equated with the fraction of sickled cells, where sickling is used to indicate any saturation-dependent deformation (Fig. 6).

Although the variation between individual patients in the properties of sickle cell blood make precise quantitative comparisons difficult, the sickling and unsickling curves (Fig. 6) as a function of oxygen pressure calculated from our data are qualitatively consistent with the results of other techniques. First, previous studies of the traditional sickling curve, measured by counting deformed cells after a 15-minute equilibration period at the final oxygen pressure and

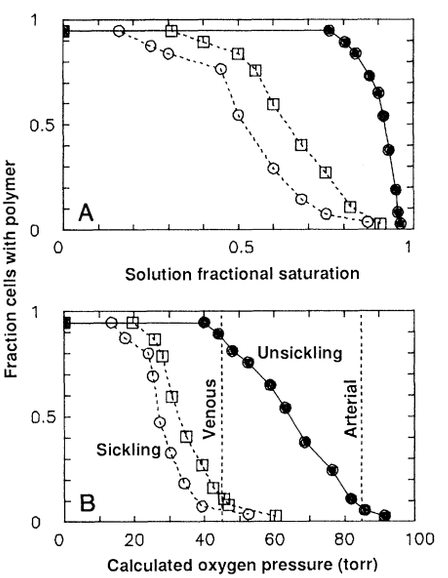

Fig. 6. Fraction of cells containing polymer as a function of saturation with carbon monoxide and calculated oxygen pressure. (**A**) Fraction of cells containing polymer as a function of fractional saturation of solution phase with carbon monoxide in photolysis experiments. This is the same data displayed in Fig. 5A. The open circles are the data from the 1-minute desaturation experiments, the open squares from the 10-minute desaturation experiments, and the filled circles from resaturation experiments. (**B**) Fraction of cells containing polymer versus calculated oxygen pressure. The oxygen pressures were calculated from the saturations in (A) with the least-squares fit of the two-state allosteric saturation function to the binding curve of normal blood (*18*) at 37°C, *p*H 7.4, pCO_2 = 40 torr with parameters $K_T = 0.0082$ torr^{-1}, $K_R = 0.95$ torr^{-1}, and $L = 3.1 \times 10^5$. The vertical dashed lines indicate the average oxygen pressure found in the arteries and veins of patients with homozygous sickle cell disease (*30*).

fixation with glutaraldehyde, gives pressures for 50 percent sickling in a study of seven patients between 32 torr and 39 torr, in excellent agreement with the value of 33 torr from our 10-minute sickling curve (*28*). A similar comparison cannot be made for unsickling curves, since there have been no previous measurements. Initial measurements, in which the shape of cells is monitored as a function of oxygen pressure by optical micrography, do show the large hysteresis in sickling and unsickling saturations observed in the photolysis experiments (*29*). Measurement of average properties of cell populations are also in qualitative agreement with our results. The persistence of polymerized hemoglobin to high saturations, predicted from solubility studies (*4, 12*), has been observed in oxygen binding curves on sickle blood (*18*), and later confirmed in slow desaturation experiments by nuclear magnetic resonance measurements (*19*).

Gelation in vivo. Our results on individual sickle cells provide new insight into the question of intracellular gelation in vivo. Some basic facts about circulatory physiology are pertinent to this discussion. The arterial oxygen pressure in sickle cell disease patients is 85 ± 8 (SD) torr [normal is 92 ± 5 (SD) torr], whereas the mixed venous pressure is 46 ± 3 (SD) torr [normal is 39 ± 0.8 (SD) torr] (*30*). In the average round trip through the circulation a red cell spends about 1 second in the alveoli of the lungs, about 3 seconds in the arterial circulation, about 1 second in the microcirculation of the tissues, and about 10 seconds in the venous return (*31*).

The unsickling curve in Fig. 6B shows that at equilibrium about 5 percent of cells contain polymer at oxygen pressures of 85 torr, while at mixed venous oxygen pressures about 85 percent of cells contain polymer at equilibrium. The situation in vivo is expected to be quite different because of the delay time prior to the onset of gelation. The present data argue that about 95 percent of cells in the arterial circulation of this patient are polymer-free, while the 1-minute sickling curve indicates that a comparable fraction of cells contain no polymer at mixed venous saturations. Our data thus suggest that in vivo approximately 80 percent of the cells are prevented from sickling in every round trip through the circulation because the delay times are so long that these cells return to the lungs before any rheologically significant polymerization has occurred. They also suggest that there is little additional sickling from deoxygenation in the microcirculation.

This analysis is oversimplified, and the actual number of sickled cells in the veins might be somewhat higher because oxygen extraction in the microcirculation of some tissues is considerably greater than the average, such as in the coronary and hepatic circulations (*32*), and the cells in these organs will have much shorter delay times. Also, the fraction of polymer-free cells in the arteries might be somewhat lower because of slow depolymerization in the lungs (*33*). The major conclusions, however, are supported by available data on the percentage of deformed cells in blood that has been fixed with glutaraldehyde immediately after withdrawal from the arteries and veins of patients. These data take on new significance in light of our results and those of the rheological study (*26*) that, with the possible exception of experiments on a subsecond time scale (*17, 34*), cell morphology can be a reliable indicator of intracellular gelation. Results from three independent studies on a total of 60 patients with homozygous sickle cell disease show that an average of about 10 percent of cells are sickled in the arteries and about 20 percent in the veins (*30, 32, 35*). In spite of some uncertainties about these data, the conclusion from these studies is clear; in agreement with the analysis of our data from the photolysis experiments (Fig. 6), most cells in both the arterial and venous circulations of sickle cell patients do not contain polymer. Another consequence of this finding is that the effect of polymerization in enhancing oxygen unloading in the tissues has been considerably overestimated, since it is based on in vitro equilibrium measurements in which much more polymer is present than in the in vivo situation (*7*). These considerations indicate that descriptions of gelation in vivo that do not include a kinetic analysis (*6, 36, 37*) are inadequate and can be misleading.

The work presented above is only the beginning of a quantitative description of the dynamics of gelation and vaso-occlusion in vivo. The scheme presented in Fig. 7 points to the need for measuring gelation and degelation at the much faster rates of deoxygenation and oxygenation found in the circulation. Our laser technique could be modified for such measurements. Such data would allow a quantitative assessment of the percentage of cells that are sickled in various locations in the microcirculation. It would also be important to develop rapid sampling techniques that could assess the extent of intracellular gelation, or at least the presence of polymer, in individual cells from arterial and venous blood.

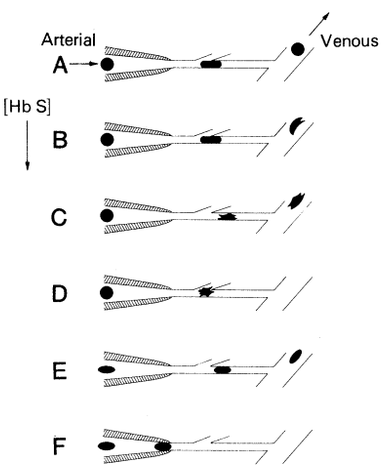

Fig. 7. Possible events occurring in the microcirculation of sickle cell patients. An arteriole, a branched capillary, and venule are shown. Cells that are polymer-free in the arterial circulation pass through the microcirculation and may reach the lungs before gelation occurs (**A**); they may undergo gelation in the venules or veins, as indicated by deformation of the cell (**B**); or they may gel in the capillaries (**C** and **D**). The probability for each of these will be determined by the delay time before gelation relative to the appropriate transit time (*7, 15*). In (A) and (B) the cells inside the capillary contain no polymer, but deform to pass through. The majority of cells are known from the analysis presented in the text to have delay times longer than 10 seconds at venous oxygen pressures and will return to the lungs and be reoxygenated before gelation occurs (A). If the delay time is between 1 and 10 seconds, gelation will occur in the venules or veins (B), and if it is about 1 second or less, gelation will occur while the cell is still in the narrow capillary (**C** and **D**). Cells that undergo gelation in the capillaries may experience an increased transit time, or produce a more permanent blockage (D) as a result of the decreased deformability. Cells may also enter the microcirculation containing variable amounts of polymer (**E** and **F**). This may occur either because the total concentration of the cell is higher than the solubility even at arterial pressures, or because depolymerization would occur at equilibrium, but requires longer than the 3 seconds that the cell resides in the arterial circulation. In these cells, deoxygenation will be accompanied by rapid gelation without a delay, as shown in the present experiments, and vaso-occlusion might occur in the arterioles (F) (*36*). From this description it is clear that the percentage of cells in the capillary circulation that are blocked in the steady state depends not only on the probability of gelation occurring in the microcirculation, but also on the rate at which occluded vessels are reopened.

REFERENCES AND NOTES

1. G. Serjeant, *Sickle Cell Disease* (Oxford Univ. Press, Oxford, 1985).
2. H. F. Bunn and B. G. Forget, *Hemoglobin: Molecular, Genetic and Clinical Aspects* (Saunders, Philadelphia, 1986).
3. S. J. Edelstein, *J. Mol. Biol.* **150**, 557 (1981); E. A. Padlan and W. E. Love, *J. Biol. Chem.* **260**, 8280 (1985).
4. H. R. Sunshine, J. Hofrichter, F. A. Ferrone, W. A. Eaton, *J. Mol. Biol.* **158**, 251 (1982).
5. F. A. Ferrone, J. Hofrichter, W. A. Eaton, *ibid.* **183**, 611 (1985).
6. C. T. Noguchi and A. N. Schechter, *Annu. Rev. Biophys. Biophys. Chem.* **14**, 239 (1985).
7. W. A. Eaton and J. Hofrichter, *Blood*, in press.
8. J. Hofrichter, P. D. Ross, W. A. Eaton, *Proc. Natl. Acad. Sci. U.S.A.* **71**, 4864 (1974).
9. R. Malfa and J. Steinhardt, *Biochem. Biophys. Res. Commun.* **59**, 887 (1974); K. Moffat and Q. H. Gibson, *ibid.* **61**, 237 (1974).
10. J. Hofrichter, P. D. Ross, W. A. Eaton, *Proc. Natl. Acad. Sci. U.S.A.* **73**, 3035 (1976).

11. H. R. Sunshine, J. Hofrichter, W. A. Eaton, *J. Mol. Biol.* **133**, 435 (1979).
12. J. Hofrichter, *ibid.* **128**, 335 (1979).
13. S. J. Gill, R. Spokane, R. C. Benedict, L. Fall, J. Wyman, *ibid.* **140**, 299 (1980).
14. F. A. Ferrone, J. Hofrichter, W. A. Eaton, *ibid.* **183**, 591 (1985).
15. W. A. Eaton, J. Hofrichter, P. D. Ross, *Blood* **47**, 621 (1976).
16. M. Seakins, W. N. Gibbs, P. F. Milner, J. F. Bertles, *J. Clin. Invest.* **52**, 422 (1973); M. E. Fabry *et al.*, *Blood* **64**, 1042 (1984); G. P. Rodgers, A. N. Schechter, C. T. Noguchi, *J. Lab. Clin. Med.* **106**, 30 (1985).
17. M. Coletta, J. Hofrichter, F. A. Ferrone, W. A. Eaton, *Nature (London)* **300**, 194 (1982).
18. R. M. Winslow, in *Biochemical and Clinical Aspects of Hemoglobin Abnormalities*, W. S. Caughey, Ed. (Academic Press, New York, 1978), p. 369.
19. C. T. Noguchi, D. A. Torchia, A. N. Schechter, *Proc. Natl. Acad. Sci. U.S.A.* 77, 5487 (1980); *J. Clin. Invest.* **72**, 846 (1983).
20. F. A. Ferrone, J. Hofrichter, H. R. Sunshine, W. A. Eaton, *Biophys. J.* **32**, 361 (1980).
21. J. Hofrichter, *J. Mol. Biol.* **189**, 553 (1986).
22. ———, J. S. Gethner, W. A. Eaton, *Biophys. J.* **24**, 20a (1978).
23. R. G. Shulman, J. J. Hopfield, S. Ogawa, *Q. Rev. Biophys.* **8**, 325 (1975); M. F. Perutz, *Nature (London)* **228**, 726 (1970); B. Shanaan, *J. Mol. Biol.* **171**, 31 (1983).
24. M. Brunori, J. Bonaventura, C. Bonaventura, E. Antonini, J. Wyman, *Proc. Natl. Acad. Sci. U.S.A.* **69**, 868 (1972).
25. C. A. Sawicki and Q. H. Gibson, *J. Biol. Chem.* **251**, 1533 (1976); V. S. Sharma, M. R. Schmidt, H. M. Ranney, *ibid.*, p. 4267; A. Szabo, *Proc. Natl. Acad. Sci. U.S.A.* **75**, 2108 (1978).
26. G. B. Nash, C. J. Johnson, H. J. Meiselman, *Blood* **67**, 110 (1986).
27. S. J. Gill, R. C. Benedict, L. Fall, R. Spokane, J. Wyman, *J. Mol. Biol.* **130**, 175 (1979).
28. R. M. Bookchin, T. Balazs, L. C. Landau, *J. Lab. Clin. Med.* **87**, 597 (1976).
29. A. Mozzarelli, unpublished results.
30. J. Lonsdorfer, P. Bogui, A. Otayeck, E. Bursaux, C. Poyart, R. Cabannes, *Bull. Eur. Physiopathol. Respir.* **19**, 339 (1983).
31. P. A. Altman and D. S. Ditmer, Eds., *Respiration and Circulation* (Federation of American Society of Experimental Biologists, Bethesda, MD, 1971).
32. W. N. Jensen, D. L. Rucknagel, W. J. Taylor, *J. Lab. Clin. Med.* **56**, 854 (1960).
33. J. P. Harrington, D. Elbaum, R. M. Bookchin, J. B. Wittenberg, R. L. Nagel, *Proc. Natl. Acad. Sci. U.S.A.* **74**, 203 (1977); M. J. Messer, J. A. Hahn, T. B. Bradley, in *Proceedings of the Symposium on Molecular and Cellular Aspects of Sickle Cell Disease*, J. I. Hercules, G. L. Cottam, M. R. Waterman, A. N. Schechter, Eds. (DHEW NIH 76-1007, Bethesda, MD, 1976), p. 225.
34. J. A. Hahn, M. J. Messer, T. B. Bradley, *Br. J. Haematol.* **34**, 559 (1976).
35. G. R. Serjeant, M. C. Petch, B. E. Serjeant, *J. Lab. Clin. Med.* **81**, 850 (1973).
36. C. T. Noguchi and A. N. Schechter, *Blood* **58**, 1057 (1981).
37. M. M. Vayo, H. H. Lipowsky, N. N. Karp, E. E. Schmalzer, S. Chien, *Microvasc. Res.* **30**, 195 (1985).
38. W. A. Eaton and J. Hofrichter, *Methods Enzymol.* **76**, 175 (1981).
39. We thank P. Griffith and A. W. Nienhuis for their cooperation in providing the continuous supply of blood samples that made this study possible and E. R. Henry for developing data analysis programs.

6 February 1987; accepted 15 June 1987